



## Research article

## Structure and phase analysis of calcium carbonate powder prepared by a simple solution method

Renny Febrida<sup>a,b,e</sup>, Setianto Setianto<sup>a,c,e</sup>, Ellyza Herda<sup>d</sup>, Arief Cahyanto<sup>b,e</sup>, I Made Joni<sup>c,e,\*</sup><sup>a</sup> Post Graduate School, Biotechnology Department, Universitas Padjadjaran, Jl. Dipati Ukur No. 35 Bandung 40132, West Java, Indonesia<sup>b</sup> Department of Dental Materials Science and Technology, Faculty of Dentistry, Universitas Padjadjaran, Jl. Raya Bandung-Sumedang KM 21, Jatinangor, Sumedang, West Java 45363, Indonesia<sup>c</sup> Department of Physics, Faculty of Mathematics and Natural Sciences, Universitas Padjadjaran, Jl. Raya Bandung-Sumedang KM. 21, Jatinangor, Sumedang, West Java 45363, Indonesia<sup>d</sup> Department of Dental Material, Faculty of Dentistry, Universitas Indonesia, Jakarta 10430, Indonesia<sup>e</sup> Functional Nano Powder University Center of Excellence, Universitas Padjadjaran, Jl. Raya Bandung-Sumedang KM 21, Jatinangor, Sumedang, West Java 45363, Indonesia

## HIGHLIGHTS

- The engineered crystal structure and phase transformation of CaCO<sub>3</sub> were achieved at room temperature using Ca(NO<sub>3</sub>)<sub>2</sub> and Na<sub>2</sub>O<sub>3</sub> precursor.
- The vaterite phase formed at 15 min and 30 min reaction times with pH ~ 7.9 shows the spherical morphologies (2–5 μm in diameter).
- Different reaction times and pH vs. formation and transformation of various CaCO<sub>3</sub> phase was demonstrated experimentally.

## ARTICLE INFO

## Keywords:

Ca(NO<sub>3</sub>)<sub>2</sub>  
calcium carbonate  
vaterite  
simple solution method

## ABSTRACT

This paper focused on the analysis of the crystal structure and phase transformation of CaCO<sub>3</sub> synthesized by simple solution method from 0.5 M Ca(NO<sub>3</sub>)<sub>2</sub> precursor and 0.5 M Na<sub>2</sub>CO<sub>3</sub> precipitant at ambient temperature (300 K). The pH of the sample solution at various reaction times of 5, 10, 15, and 30 min were measured and correlated with the supersaturating condition in the presence of the Na<sub>2</sub>CO<sub>3</sub> which is responsible for vaterite phase formation. The formation of the polymorph structure of obtained CaCO<sub>3</sub> powders was characterized using powder X-ray diffraction patterns and their crystal structure and phase transformation were evaluated using the Rietveld refinement method. Moreover, the qualitative analysis of the CaCO<sub>3</sub> powders phase was conducted by Fourier Transform Infrared (FTIR) spectroscopy to evaluate the effect of reaction time correlated with their crystal formation. The XRD analysis showed that the vaterite formation was 89 % at a reaction time of 15 min and confirmed also by FTIR that the amount of vaterite increased due to the effect of increasing reaction time. The crystallite size of vaterite was stable at 36 nm at the reaction time of 15 and 30 min. The morphology of the CaCO<sub>3</sub> powders obtained from Scanning Electron Microscope (SEM) was spherical with sizes of 2–5 μm. It was highlighted that the supersaturating condition started occurred at a reaction time of 15 min at pH 7.88 which was responsible for vaterite formation took place. It was concluded that the amount of precipitant (Na<sub>2</sub>CO<sub>3</sub>) and reaction times play an important role to determine the saturation of carbonate source to allow vaterite phase formation of CaCO<sub>3</sub> powders to occur.

## 1. Introduction

Calcium carbonate (CaCO<sub>3</sub>) is an abundant inorganic biomaterial in the manner of different structures (calcite, vaterite, and aragonite) [1, 2]. Thermodynamically, the form of CaCO<sub>3</sub> under normal conditions is

β-CaCO<sub>3</sub> (calcite). Other polymorphs of CaCO<sub>3</sub> such as λ-CaCO<sub>3</sub> (aragonite) and μ-CaCO<sub>3</sub> (vaterite) can be formed at certain synthesis temperatures [3]. The applications of CaCO<sub>3</sub> as a biomaterial are strongly dependent on their structure and phase transformation to become a concern of researchers in various fields. This material is increasingly used

\* Corresponding author

E-mail address: [imadejoni@phys.unpad.ac.id](mailto:imadejoni@phys.unpad.ac.id) (I.M. Joni).<https://doi.org/10.1016/j.heliyon.2021.e08344>

Received 3 March 2021; Received in revised form 14 July 2021; Accepted 4 November 2021

2405-8440/© 2021 The Author(s). Published by Elsevier Ltd. This is an open access article under the CC BY-NC-ND license (<http://creativecommons.org/licenses/by-nc-nd/4.0/>).

in many industries (i.e. in paint, rubber, plastics, and biomaterials) since its physical and chemical properties can be engineered [4, 5, 6, 7, 8].

The process of  $\text{CaCO}_3$  crystals formation usually takes place in three important steps. Initially, the formation of amorphous calcium carbonate (ACC) begins, which then turns into calcite and vaterite phases at low temperatures (14–30 °C), while at 60–80 °C it becomes calcite and aragonite. In the third stage, the composition of vaterite and aragonite decreases along with the increase in calcite formation [9]. The formation of polymorphic  $\text{CaCO}_3$  crystals results in different particle morphology. Calcite has a rhombohedral shape, aragonite has a needle-like particle shape, whereas vaterite has a spherical shape [10].

The polymorph structure and their morphology of  $\text{CaCO}_3$  powder achieve by various synthesis techniques such as deposition of homogeneous solutions [11], water in oil in water emulsion [12, 13], mechano-chemical and sonochemical synthesis [14, 15], water-in-oil (W/O) microemulsion [16, 17], and high-pressure homogenizer (HPH) [7]. The standard engineering of  $\text{CaCO}_3$  polymorphs, tuned shapes, and sizes are obtained by controlling over crystal growth mechanism [9]. The mechanism of vaterite crystal growth approaches is widely investigated and adopted by many researchers to synthesis vaterite crystals using additives such as organic additives and/or organic polymers to control the crystal growth, i.e. [10, 18, 19]. The influence of additives on the rate of  $\text{CaCO}_3$  was reported by many researchers [19, 20, 21, 22]. A high concentration of mixed solvents of ethylene glycol and water affected the polymorphic composition and favoured the precipitation of the vaterite phase. The addition of ethylene glycol may reduce the  $\text{CaCO}_3$  precipitation rate. In this condition, high supersaturation was preserved for a longer time and resulted in a higher concentration of vaterite phase, probably as a result of kinetic stabilization by slowing the growth rate of the more stable polymorphs [22]. Other researcher reports additional amino acids (glycine) to obtain the vaterite phase in the synthesis by precipitation process [23]. Recently reported that mesoporous vaterite  $\text{CaCO}_3$  crystals synthesized by simple solution method without additive by mixing of  $\text{Ca}^{2+}$  and  $\text{CO}_3^{2-}$  salts in aqueous media from  $\text{Na}_2\text{CO}_3$  and  $\text{CaCl}_2$  precursor [24].

Moreover, the polymorphism of the obtained  $\text{CaCO}_3$  powder depends also on the chosen precursors. Most reported research uses Calcium Chloride ( $\text{CaCl}_2$ ) as a salt precursor as a source of calcium ions [25] and Sodium carbonate ( $\text{Na}_2\text{CO}_3$ ) or potassium carbonate  $\text{K}_2\text{CO}_3$  as anions source [26]. The advantage of  $\text{CaCl}_2$  is very easily dissolved in water to generate calcium ions and react with the carbonate source to form a solid precipitate of calcium carbonate due to an exothermic process [27]. However, governing the crystal growth in the exothermic process is quite difficult without controlling the temperature. Also, irregular cubic particles are obtained when the crystal growth process by stirring the solution for a longer time [28]. Another important factor that affects the formation of  $\text{CaCO}_3$  polymorphs is the pH of the solution during the precipitation process. At particular temperature and concentration of the solution. At 24 °C and a low concentration of  $\text{CaCl}_2$  solution (0.0134 M), pure calcite is obtained at a pH of more than 12, aragonite is obtained at a pH of 11, and vaterite is obtained at a pH less than 10 [29]. Mitsuki Kogo et. all [30] reported the adjustment of the pH from 2.0–11.3 to the initial pH of 0.1 M  $\text{CaCl}_2$  and  $\text{NaCO}_3$  solution of 6.5 by adding HCl and  $\text{NH}_3$  to investigate the polymorph process. From the result of X-ray diffraction, single-phase vaterite is formed at initial pH 2.5 with spherical shape and particle size of 1–10  $\mu\text{m}$  [30]. In contrast, Radek Ševčík et. all obtain high pure vaterite (99 wt%) from high concentration solution (2 M  $\text{CaCl}_2$  precursor and  $\text{K}_2\text{CO}_3$  precipitant) provided higher temperature (60 °C) and higher stirring speed of 600 rpm [31]. However, the morphology of the obtained particles are irregular in shape and mainly as big bodies up to 10  $\mu\text{m}$  in size may be due to massive crystallization of many nuclei that joined together during growth at high concentrations of the solution. To the best knowledge of the author and review from reported research, the use of calcium nitrate  $\text{Ca}(\text{NO}_3)_2$  as a source of cations is rarely used as a precursor for  $\text{CaCO}_3$  synthesis. Interestingly, the reaction of  $\text{Ca}(\text{NO}_3)_2$  in water is endothermic consequently no need for effort to control the temperature process if compared to  $\text{CaCl}_2$ .

Recently, the fabrication of  $\text{CaCO}_3$  crystals with sizes beyond the conventional range without additives is still a challenge [24]. Our current study provides the polymorphic transformation from calcite stable phase to vaterite metastable phase without any additives and templates by a simple method. In this study, we analyzed the crystal structure and phase transformation of  $\text{CaCO}_3$  synthesized by simple solution method from  $\text{Ca}(\text{NO}_3)_2$  precursor and  $\text{Na}_2\text{CO}_3$  precipitant. The crystal structure and phase transformation were analyzed using the Rietveld refinement method [32]. This method is a sophisticated procedure for quantitative analysis of  $\text{CaCO}_3$  powder containing a mixture of calcite and vaterite from powder X-ray diffraction (XRD) data at various reaction times. The investigation on the structure and phase transformation also correlated with the pH of the solution at various reaction times. The final particles are spherical in shape with porous morphology. The formation of porous polycrystalline vaterite was markedly different from the conventional particle to particle formation in which nucleation occurred.

## 2. Material and method

### 2.1. Material

In this research, all of the materials we use are high-quality commercial products. Sodium carbonate ( $\text{Na}_2\text{CO}_3$ ) and calcium nitrate tetrahydrate ( $\text{Ca}(\text{NO}_3)_2 \cdot 4\text{H}_2\text{O}$ ) were purchased from Merck (Indonesia).

### 2.2. Synthesis of $\text{CaCO}_3$ powder

The synthesis of  $\text{CaCO}_3$  by a simple solution method is schematically shown in Figure 1. Since higher mixing temperature might initiate the formation of aragonite and calcite phases [6], the favoured range of temperatures for vaterite phase precipitation in various experiments is up to 40 °C [26]. In the current study, the temperature of 27 °C has been chosen for the experiment by mixing the solutions under 800 rpm to obtain homogenous, high-shear, and sufficient agitation to enable vaterite phase precipitation.

The calcium carbonate synthesis process started by mixing between 0.5 M  $\text{Na}_2\text{CO}_3$  and 0.5 M  $\text{Ca}(\text{NO}_3)_2 \cdot 4\text{H}_2\text{O}$  solutions. The solution was mixed continuously at a temperature of 27 °C ( $T = 300\text{ K}$ ), with the fixed stirring speed at 800 rpm with different reaction times (5, 10, 15, and 30 min). The solution was filtered to get the precipitated powder. The obtained powder was washed with ethanol to remove the remaining contaminant indicated by the white appearance of the powder. The powder was then dried in a vacuum desiccator for 48 h and subjected to analysis. The pH of the initial solution (0 min) and after the reaction time at various reaction times (5, 10, 15, and 30 min) was measured as a parameter in the formation of the structure and phase of the  $\text{CaCO}_3$  powder.

### 2.3. Characterizations

We used X-ray diffraction measurements (PANalytical) to analyze the crystal structure of the synthesized  $\text{CaCO}_3$  powder. Data were collected over a 2-theta in the range of 20–80° with a time step of 2.90 s.  $\text{Cu-K}\alpha$  X-ray radiation at a wavelength of 1.5406 Å was used. Synthesized  $\text{CaCO}_3$  powders were measured using Fourier Transform Infrared Spectroscopy (FTIR, Nicolet iS5, Thermo Scientific) to determine the vibration mode. The measured infrared spectrum region was in the range 600–1000  $\text{cm}^{-1}$  represented the fingerprint area that was used in analyzing the polymorphous vibration mode of the synthesized  $\text{CaCO}_3$  powder [33]. The scanning electron microscope (SEM, Hitachi SU3500) with an accelerating voltage of 10 kV was used to characterize the morphology of  $\text{CaCO}_3$  powders. The morphology of obtaining  $\text{CaCO}_3$  powder used to identify the shape of the particle at various reaction times indicated the presence of rhombohedral (calcite) and spherical (vaterite) shapes.

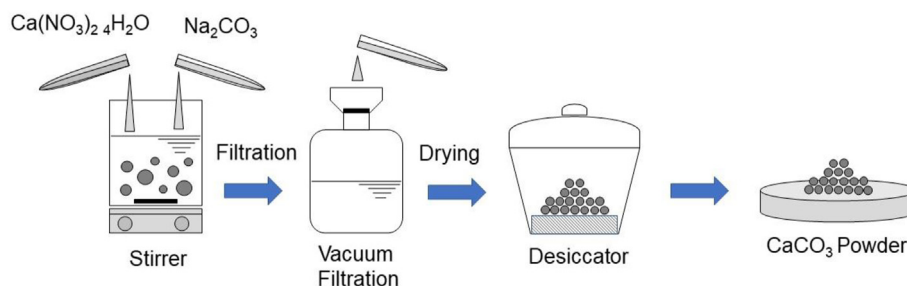


Figure 1. Schematic illustration of synthesis  $\text{CaCO}_3$  by simple solution method.

#### 2.4. Crystal structure analysis and phase identification

The structural analysis including the crystallite size and phase identification of the synthesized powder employed open-source software, MAUD [34]. We used the crystal structure of calcite as trigonal [35] and the vaterite is orthorhombic [36] in the entire analysis. The unit cells of calcite and vaterite are represented three-dimensionally by the atoms of each crystal as shown in Figure 2 were visualized by the VESTA software package [37]. The detailed quantitative results based on Rietveld refinement method analysis were then used for crystallite size calculation using the Scherrer method [38]. Qualitative analysis of the synthesized  $\text{CaCO}_3$  powder was carried out by comparing the vibration bending mode ratio between the vaterite phase in the  $744\text{ cm}^{-1}$  area and calcite which was located at the wave number  $711\text{ cm}^{-1}$  [39].

### 3. Results and discussions

#### 3.1. Structural analyses of $\text{CaCO}_3$ powder

The XRD pattern of the polymorphs of  $\text{CaCO}_3$  is shown in Figure 3. The XRD patterns characteristic peaks corresponding to the stable phase (calcite) and metastable phase (vaterite) were observed at  $T = 300\text{ K}$  in various reaction times from 5–30 min. It was observed the transformation of the calcite phase to the vaterite phase occurred at various reaction times. When the reaction time for calcium carbonate precipitation was only 5 min, the majority of the crystals formed were calcite (94%) and contained only a small phase of vaterite (6%). After the reaction time was increased to 10 min, the precipitate contained a mixture of calcite (52%) and vaterite (48%) crystals. It showed that dissolution re-precipitation was occurred to form polymorph crystal of calcium carbonate [40]. At the reaction time of 15 min, it provided a condition to create the new solid particles, i.e., vaterite (90%) as a major phase and calcite (10%) as a secondary phase. This result indicated that reaction time 15 min appropriate condition to form calcium carbonate precipitate with a vaterite crystal structure. In 30 min of reaction time, the vaterite phase was

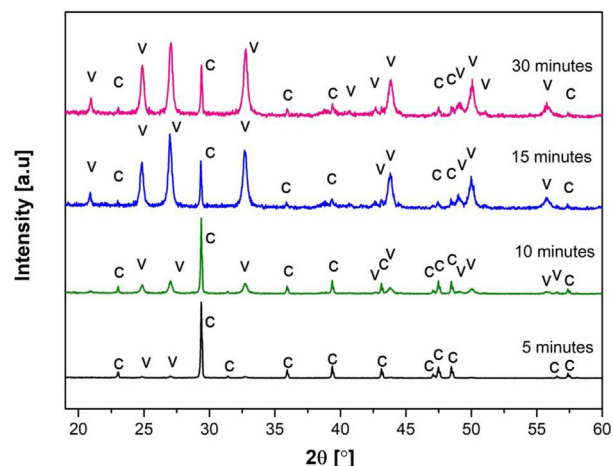


Figure 3. XRD patterns of synthesized  $\text{CaCO}_3$  powder at various reaction times.

decreased slightly (89%) due to the crystal formation process of a stable phase of calcite about 11%. In conclusion, the major calcite phase was obtained rapidly at 5 min of reaction times, and we could find the appropriate reaction time of the vaterite phase at 15 min, and it was highlighted the reaction occurred at room temperature.

The crystallite sizes of calcite decreased significantly due to the defects that occurred in the transformation process (Table 1). While the crystallite sizes of vaterite showed only slight changes. The result described that the crystallite size for both calcite and vaterite were stable occurred at the reaction time of 15 and 30 min. The characteristic of crystal also determined by the volume of unit cell represented of the density of the unit cell might be affected by reaction time. The effect of reaction time on the formation of  $\text{CaCO}_3$  precipitation on the unit cell volume of calcite and vaterite crystals phase was shown in Table 2. At the reaction time of 5 min, the volume of the unit cell of the two crystals

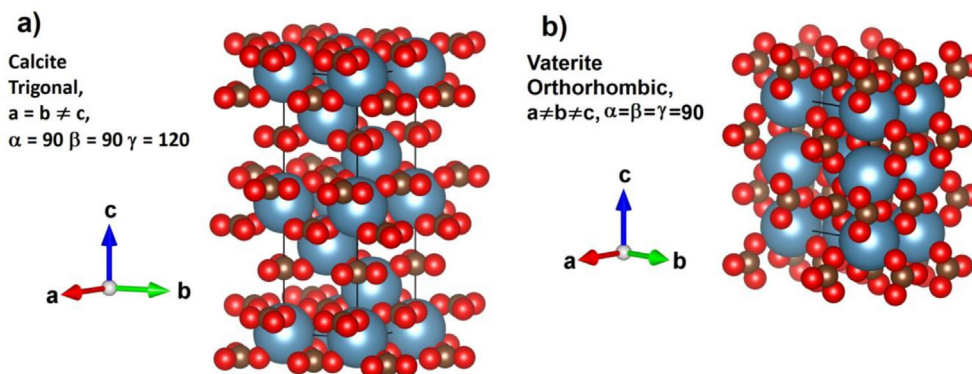


Figure 2. Space-filling representation of the crystal structure of trigonal calcite (a) and orthorhombic vaterite (b) in three dimensional lattice vectors; blue, brown and red sphere represent Ca atom, C atom, and O atom.

**Table 1.** Quantitative analysis of crystal structure and phase of synthesized CaCO<sub>3</sub> powder at various reaction time.

Reaction time (minutes)	Calcite (wt%) Trigonal, a = b ≠ c, α = 90 β = 90 γ = 120	Vaterite (wt%) Orthorhombic, a ≠ b ≠ c, α = β = γ = 90	Calcite Crystallite size (nm) (Scherrer)	Vaterite Crystallite size (nm) (Scherrer)
5	93.55; a = 4.99; c = 17.06	6.45; a = 4.13; b = 7.15; c = 8.48	(106.36)	(42.97)
10	51.53; a = 4.99; c = 17.06	48.47; a = 4.13; b = 7.15; c = 8.46	(100.12)	(29.02)
15	10.21; a = 4.99; c = 17.05	89.79; a = 4.12; b = 7.15; c = 8.46	(83.04)	(36.19)
30	11.37; a = 4.99; c = 17.05	88.63; a = 4.13; b = 7.14; c = 8.47	(87.03)	(36.28)

**Table 2.** Unit cell volume of synthesized CaCO<sub>3</sub> powder at various reaction time.

Reaction times (minutes)	Calcite Unit Cell volume (Å <sup>3</sup> )	Vaterite Unit Cell volume (Å <sup>3</sup> )
Ref. data (AMCSD)	367.9162	250.4102
5	367.9314	250.4102
10	367.6289	249.7856
15	367.1829	249.3785
30	367.4410	249.6451

(calcite and vaterite) was still close to reference [35, 36]. The smallest of the unit cell volume for both calcite and vaterite were formed at the reaction time of 15 min. Theoretically, we know that the volume of the unit cell is inversely proportional to the density of the unit cell. Thus, we conclude that the highest density of calcite and vaterite unit cells occurred at the reaction time of 15 min.

### 3.2. Vibrational mode analyses

Infrared spectroscopy serves as a useful tool to study different calcium carbonate phases (calcite, aragonite, and vaterite) since each phase shows characteristic absorption bands in its infrared spectrum [33]. The regions of the absorption bands corresponding to the two fundamental vibrational modes of carbonate ion at ~700 cm<sup>-1</sup> (in-plane bending, ν<sub>4</sub>) and 877 cm<sup>-1</sup> (out of plane bending, ν<sub>2</sub>) are assigned [31]. The ν<sub>4</sub> band at ~700 cm<sup>-1</sup> is a fingerprint region and distinct for crystalline phases (calcite, aragonite, and vaterite) provides useful information for CaCO<sub>3</sub> polymorph assignment. The FTIR spectroscopy of CaCO<sub>3</sub> powder is shown in Figure 4. For precipitated CaCO<sub>3</sub> samples with a reaction time of 5 min, the absorption peak of calcite was observed at 711 cm<sup>-1</sup>. The weak ν<sub>2</sub> band at 877 cm<sup>-1</sup> for calcite indicate defective crystal structure [41]. The absorption peaks at 711 and 744 cm<sup>-1</sup> were assigned for mixture calcite-vaterite precipitate at reaction time reach up to 10 min. At the prolonged reaction time (10–30 min), the phases of vaterite (ν<sub>4</sub> band at 744 cm<sup>-1</sup>) was increased, while the ν<sub>4</sub> band for calcite at 711

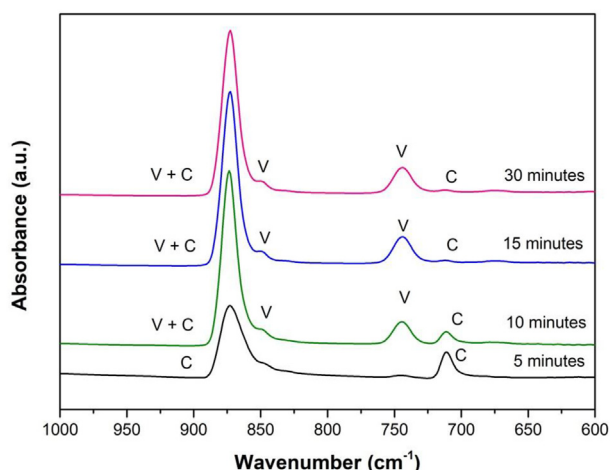
cm<sup>-1</sup> was suppressed. The concentration ratio of vaterite–calcite in the calcium carbonate samples from FTIR spectra can be determined by using the absorbance peak ratio at ν<sub>4</sub> band which was given in Table 3. Qualitatively, the amount of vaterite increased due to the effect of increasing reaction time. It was shown that the optimum reaction time for the vaterite phase had occurred at 15 min.

### 3.3. Morphology of CaCO<sub>3</sub> powder

The morphology of CaCO<sub>3</sub> powder which was influenced by the reaction time was shown in a grayscale image showing the topography of the sample in Figure 5a–d in a combination of rhombohedral and spherical particles [42]. Figure 5a indicated that the calcium carbonate precipitate was a rhombohedral shape, which was the morphology of calcite. Figure 5b, rhombohedral calcite particles, and spherical vaterite particles were precipitated. This occurred because the reaction time was increased up to 10 min, the saturation level of calcium carbonate increases so that the shape becomes irregular, calcite–vaterite mixture. The calcite phase started to decrease with increasing reaction time and the vaterite phase started to appear. Figure 5c, the morphology of the calcium carbonate precipitate started to be spherical but still showed a rough surface. Under this condition, the majority of the powders synthesized were shown to be in the vaterite phase. In Figure 5d, the calcium carbonate precipitated were spherical with a smoother surface, which indicated the reaction time was appropriate for vaterite crystal growth. The SEM images showed that the synthesized CaCO<sub>3</sub> powders were spherical in shape with sizes of 2–5 μm. More spherical vaterite particles obtained at 15 and 30 min reaction times (Figure 5) confirmed the presence of the vaterite phase as the dominant phase obtained from XRD quantitative analysis (Figure 3). The presence of the rhombohedral calcite phase was also remarkably reduced. Our results are consistent with the work studied by Baqiya et al. [43]. They found that when the weight fraction of the vaterite phase is quite high (~95%), the particles tend to have spherical morphology due to a decrease of concentration between CO<sub>3</sub><sup>2-</sup> and Ca<sup>2+</sup> which may be the reason for the formation of the vaterite phase.

TEM analysis confirmed morphology of obtained vaterite microstructure as shown in Figure 6. The TEM images showed the CaCO<sub>3</sub> microsphere consisted of primary particles with relatively homogeneous in size around 150 nm.

A multipoint BET measurement was conducted. BJH (Barret, Joyner, and Halenda) method was conducted to calculate pore surface area, pore size from experimental isotherm using adsorption and desorption technique. Only BJH desorption results were shown in the table as the desorption technique gives a narrower pore size distribution than the adsorption technique. BET analysis proved the presence of porous

**Figure 4.** FTIR of synthesized CaCO<sub>3</sub> powder at various reaction times.**Table 3.** The bending mode vibration of absorbance ratio of synthesized CaCO<sub>3</sub> powder at various reaction times.

Reaction time (minutes)	A <sub>744</sub> /A <sub>711</sub> ratio
5	0.3385
10	1.4803
15	3.4225
30	3.1540



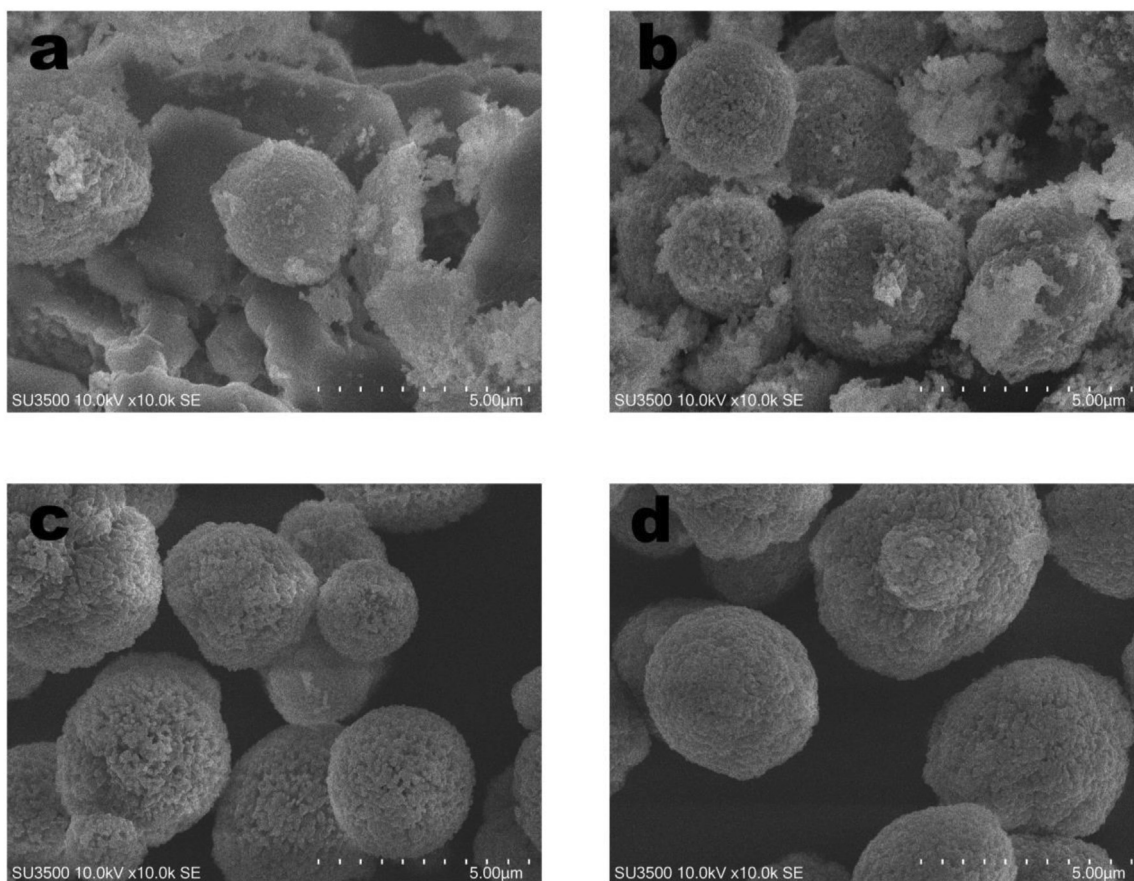


**Figure 5.** SEM images of synthesized  $\text{CaCO}_3$  particles at various reaction times (a) 5 min, (b) 10 min, (c) 15 min, (d) 30 min.

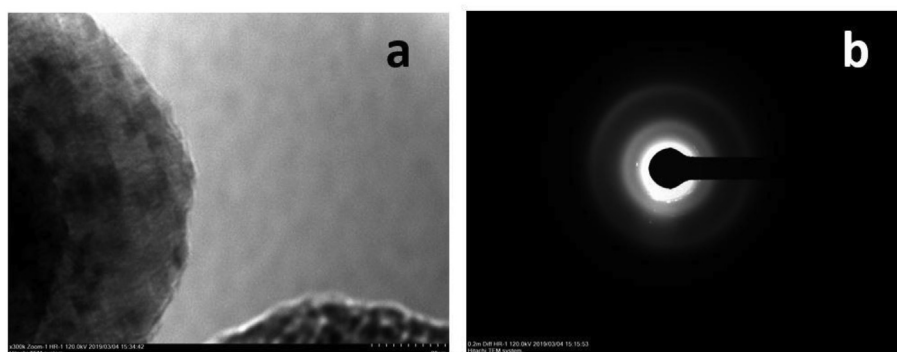


**Figure 6.** TEM (a) and SAED (b) images of synthesized  $\text{CaCO}_3$  particles at 30 min reaction time.

particles that correspond to the particle as shown in the SEM image (Figure 5). The particles possess an average pore diameter in the size of 3.58 nm, which is typical for the vaterite phase [24]. The particles possess a specific surface area of  $10.33 \text{ m}^2\text{g}^{-1}$ . This result confirmed the polymorphic transformation from calcite stable phase to vaterite metastable phase without any additives and templates.

The analysis of crystal structure and phase transformation, and morphology of  $\text{CaCO}_3$  powder at various reaction times in agreement with the pH solution parameter of carbonate formation is shown in Figure 7. The initial pH of the solution was 10.2 indicated that constituent precursors were well dissolved. At 5 min reaction time, the pH of the solution was 8.76. In this condition, the  $\text{CaCO}_3$  powder was predominantly calcite in the form of rhombohedral particles. At 10 min reaction time, the pH of the solution was 8.1 indicate the mixture of calcite-vaterite. It was highlighted that when the pH solution dropped closer

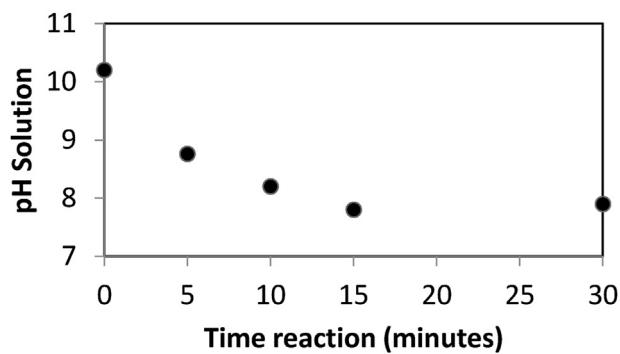


**Figure 7.** The pH of the solution at various reaction times (5–30 min).

to 7.9, which occurred at reaction time of 15 and 30 min the vaterite phase dominated as shown in the crystal structure analysis with a spherical particle shape as shown in SEM image (Figure 5c and d). Prolonged reaction time resulted in higher supersaturated solution due to high-shear and constant agitation of reactant solutions. The high supersaturation in the pH range (~7.9) helps to trap kinetically the metastable vaterite, preventing its transformation into calcite stable phase [44]. According to Ostwald's step rule [45], at higher supersaturation, the difference between interfacial energy of polymorphs is prevalent and the metastable vaterite will be formed predominantly. Our result was well aligned with Han et al. result [46] which showed that an increase in the pH value (above 8) resulted in a decrease in the vaterite concentration. When pH decreased from 9.7 to 7.7, almost pure vaterite was produced.

#### 4. Conclusions

We have successfully analyzed the crystal structure and phase transformation of CaCO<sub>3</sub> synthesized by simple solution method at room temperature (T = 300 K) using a Ca(NO<sub>3</sub>)<sub>2</sub> and Na<sub>2</sub>CO<sub>3</sub> as a precursor. The vaterite phase was formed within the reaction time of 15 and 30 min at alkaline pH ~ 7.9 with spherical morphology (2–5 μm) in diameter. In our general conclusion, the analysis of crystal structure and phase transformation of the synthesized CaCO<sub>3</sub> powder can be utilized to investigate the formation of various carbonate at different reaction times and pH of the solution.

#### Declarations

##### Author contribution statement

Renny Febrida: Conceived and designed the experiments; Performed the experiments; Analyzed and interpreted the data; Wrote the paper.

Setianto Setianto: Performed the experiments; Analyzed and interpreted the data; Contributed reagents, materials, analysis tools or data; Wrote the paper.

Ellyza Herda: Conceived and designed the experiments; Wrote the paper.

Arief Cahyanto: Analyzed and interpreted the data; Wrote the paper.

I Made Joni: Conceived and designed the experiments; Analyzed and interpreted the data; Contributed reagents, materials, analysis tools or data; Wrote the paper.

##### Funding statement

This work was supported by Universitas Padjadjaran, Academic Leadership Grant and RDDU Project 2020 (1427/UN6.3.1/LT/2020).

##### Data availability statement

Data included in article/supplementary material/referenced in article.

##### Declaration of interests statement

The authors declare no conflict of interest.

##### Additional information

No additional information is available for this paper.

#### References

1. L. Addadi, S. Raz, S. Weiner, Taking advantage of disorder: amorphous calcium carbonate and its roles in biomineralization, *Adv. Mater.* 15 (2003) 959–970.
2. L. A. S. Weiner, A pavement of pearl, *Nature* 389 (1997) 912–915.
3. R. Ropp, *Encyclopedia of the Alkaline Earth Compounds*, first ed., 2013.
4. J. Campbell, G. Kastania, D. Volodkin, Encapsulation of low-molecular-weight drugs into polymer multilayer capsules templated on vaterite CaCO<sub>3</sub> crystals, *Micromachines* 11 (2020).
5. D. Zhao, C.Q. Wang, R.X. Zhuo, S.X. Cheng, Modification of nanostructured calcium carbonate for efficient gene delivery, *Colloids Surf. B Biointerfaces* 118 (2014) 111–116.
6. Y. Ueno, H. Futagawa, Y. Takagi, A. Ueno, Y. Mizushima, Drug-incorporating calcium carbonate nanoparticles for a new delivery system, *J. Contr. Release* 103 (2005) 93–98.
7. H. Casanova, L.P. Higuita, Synthesis of calcium carbonate nanoparticles by reactive precipitation using a high-pressure jet homogenizer, *Chem. Eng. J.* 175 (2011) 569–578.
8. S. Biradar, P. Ravichandran, R. Gopikrishnan, V. Goornavar, J.C. Hall, V. Ramesh, S. Baluchamy, R.B. Jeffers, G.T. Ramesh, Calcium carbonate nanoparticles: synthesis, characterization and biocompatibility, *J. Nanosci. Nanotechnol.* 11 (2011) 6868–6874.
9. T. Ogino, T. Suzuki, K. Sawada, The formation and transformation mechanism of calcium carbonate in water, *Geochem. Cosmochim. Acta* 51 (1987) 2757–2767.
10. K.K. Sand, J.D. Rodriguez-Blanco, E. Makovicky, L.G. Benning, S.L.S. Stipp, Crystallization of CaCO<sub>3</sub> in water-Alcohol mixtures: spherulitic growth, polymorph stabilization, and morphology change, *Cryst. Growth Des.* 12 (2012) 842–853.
11. G. Yan, L. Wang, J. Huang, The crystallization behavior of calcium carbonate in ethanol/water solution containing mixed nonionic/anionic surfactants, *Powder Technol.* 192 (2009) 58–64.
12. G.X. Wu, J. Ding, J.M. Xue, Synthesis of calcium carbonate capsules in water-in-oil-in-water double emulsions, *J. Mater. Res.* 23 (2008) 140–149.
13. R. Gupta, Synthesis of Precipitated Calcium Carbonate Nanoparticles Using Modified Emulsion Membranes, *Undefined*, 2004.
14. T.A. Hassan, V.K. Rangari, S. Jeelani, Sonochemical synthesis and characterisation of bio-based hydroxyapatite nanoparticles, *Int. J. Nano Biomaterials (IJNB)* 5 (2014) 103–112.
15. S.J.T. Hassan dan, Mechanochemical and sonochemical synthesis of bio-based nanoparticles, *Proc. Nanotechnol. Conf.* (2010) 278–281.
16. M.A. Malik, M.Y. Wani, M.A. Hashim, Microemulsion method: a novel route to synthesize organic and inorganic nanomaterials. *1st Nano Update*, Arab. J. Chem. 5 (2012) 397–417.
17. A. Georgieva, B. Bogdanov, Z. Stefanov, D. Koleva, Microemulsion water-in-oil (W/O) - microreactor for synthesis of ultrafine carbonate nanostructures, *Technol. Stud.* 1 (2011) 9–13.
18. A.W. Xu, W.F. Dong, M. Antonietti, H. Cölfen, Polymorph switching of calcium carbonate crystals by polymer-controlled crystallization, *Adv. Funct. Mater.* 18 (2008) 1307–1313.
19. E.M. Flaten, M. Seiersten, J.P. Andreassen, Growth of the calcium carbonate polymorph vaterite in mixtures of water and ethylene glycol at conditions of gas processing, *J. Cryst. Growth* 312 (2010) 953–960.
20. Q. Li, Y. Ding, F. Li, B. Xie, Y. Qian, Solvothermal growth of vaterite in the presence of ethylene glycol, 1,2-propanediol and glycerin, *J. Cryst. Growth* 236 (2002) 357–362.
21. Y. Chen, X. Ji, X. Wang, Microwave-assisted synthesis of spheroidal vaterite CaCO<sub>3</sub> in ethylene glycol-water mixed solvents without surfactants, *J. Cryst. Growth* 312 (2010) 3191–3197.
22. E.M. Flaten, M. Seiersten, J.P. Andreassen, Polymorphism and morphology of calcium carbonate precipitated in mixed solvents of ethylene glycol and water, *J. Cryst. Growth* 311 (2009) 3533–3538.
23. R. Salomão, L.M.M. Costa, G.M. de Olyveira, Precipitated calcium carbonate nanoparticles: applications in drug delivery, *Adv. Tissue Eng. Regen. Med. Open Access* 3 (2017) 336–340.
24. A. Vikulina, J. Webster, D. Voronin, E. Ivanov, R. Fakhru'llin, V. Vinokurov, D. Volodkin, Mesoporous additive-free vaterite CaCO<sub>3</sub> crystals of untypical sizes: from submicron to Giant, *Mater. Des.* 197 (2021) 109220.
25. L. Guo, W. Gu, C. Peng, W. Wang, Y.J. Li, T. Zong, Y. Tang, Z. Wu, Q. Lin, M. Ge, G. Zhang, M. Hu, X. Bi, X. Wang, M. Tang, A comprehensive study of hygroscopic properties of calcium- and magnesium-containing salts: implication for hygroscopicity of mineral dust and sea salt aerosols, *Atmos. Chem. Phys. Discuss.* (2018) 1–37.
26. D. Konopacka-Lyskawa, Synthesis methods and favorable conditions for spherical vaterite precipitation: a review, *Crystals* (2019) 9.
27. R. Kemp, S.E. Keegan, Calcium Chloride, in: *Ullmann's Encycl. Ind. Chem.*, Wiley-VCH Verlag GmbH & Co. KGaA, Weinheim, Germany, 2000.
28. J. Song, R. Wang, Z. Liu, H. Zhang, Preparation and characterization of calcium carbonate microspheres and their potential application as drug carriers, *Mol. Med. Rep.* 17 (2018) 8403–8408.
29. R. Chang, S. Kim, S. Lee, S. Choi, M. Kim, Y. Park, Calcium carbonate precipitation for CO<sub>2</sub> storage and utilization: a review of the carbonate crystallization and polymorphism, *Front. Energy Res.* 5 (2017) 1–12.
30. M. Kogo, T. Umegaki, Y. Kojima, Effect of pH on formation of single-phase vaterite, *J. Cryst. Growth* 517 (2019) 35–38.
31. R. Ševčík, M. Pérez-Estébanez, A. Viani, P. Šašek, P. Mácová, Characterization of vaterite synthesized at various temperatures and stirring velocities without use of additives, *Powder Technol.* 284 (2015) 265–271.
32. H.M. Rietveld, A profile refinement method for nuclear and magnetic structures, *J. Appl. Crystallogr.* 2 (1969) 65–71.
33. L. Pérez-Villarejo, F. Takabait, L. Mahtout, B. Carrasco-Hurtado, D. Eliche-Quesada, P.J. Sánchez-Soto, Synthesis of vaterite CaCO<sub>3</sub> as submicron and nanosized particles using inorganic precursors and sucrose in aqueous medium, *Ceram. Int.* 44 (2018) 5291–5296.

- [34] L. Lutterotti, Maud: a Rietveld analysis program designed for the internet and experiment integration, *Acta Crystallogr. Sect. A Found. Crystallogr.* 56 (2000) s54.
- [35] D.L. Graf, Crystallographic tables for the rhombohedral carbonates, *Am. Mineral.* 46 (1961) 1283–1316.
- [36] Y.H.J. Meyer, Struktur und Fehlordnung des Vaterits \*, 1969.
- [37] K. Momma, F. Izumi, VESTA 3 for three-dimensional visualization of crystal, volumetric and morphology data, *J. Appl. Crystallogr.* 44 (2011) 1272–1276.
- [38] A.L. Patterson, The scherrer formula for X-ray particle size determination, *Phys. Rev.* 56 (1939) 978–982.
- [39] D. Konopacka-Lyskawa, N. Czaplicka, B. Kościelska, M. Łapiński, J. Gębicki, Influence of selected saccharides on the precipitation of calcium-vaterite mixtures by the CO<sub>2</sub> bubbling method, *Crystals* (2019) 9.
- [40] M. Farhadi Khouzani, D.M. Chevrier, P. Güttlein, K. Hauser, P. Zhang, N. Hedin, D. Gebauer, Disordered amorphous calcium carbonate from direct precipitation, *CrystEngComm* 17 (2015) 4842–4849.
- [41] P. Yin, IR - Spectroscopic Investigations of the Kinetics of Calcium Carbonate Precipitation, 2016.
- [42] K. Henzler, E.O. Fetisov, M. Galib, M.D. Baer, B.A. Legg, C. Borca, J.M. Xto, S. Pin, J.L. Fulton, G.K. Schenter, N. Govind, J. Ilja Siepmann, C.J. Mundy, T. Huthwelker, J.J. De Yoreo, Supersaturated calcium carbonate solutions are classical, *Sci. Adv.* 4 (2018) 1–12.
- [43] M.A. Baqiya, Q. Lailiyah, A. Riyanto, Z. Arifin, Triwikantoro, M. Zainuri, S. Pratapa, Darminto, Precipitation process of CaCO<sub>3</sub> from natural limestone for functional materials, *J. AOAC Int.* 103 (2020) 373–381.
- [44] I. Udrea, C. Capat, E.A. Olaru, R. Isopescu, M. Mihai, C.D. Mateescu, C. Bradu, Vaterite synthesis via gas-liquid route under controlled pH conditions, *Ind. Eng. Chem. Res.* 51 (2012) 8185–8193.
- [45] W. Ostwald, *Lehrbuch Fur Allgemeine Chemie*, Engelmann, Leipzig, Germany, 1902.
- [46] Y. Sheng Han, G. Hadiko, M. Fuji, M. Takahashi, Crystallization and transformation of vaterite at controlled pH, *J. Cryst. Growth* 289 (2006) 269–274.